X-BAND POLARIMETRIC SYNTHETIC APERTURE RADAR IMAGING OF A SMALL TREE

Makoto MURASE, Yoshio YAMAGUCHI, Hiroyoshi YAMADA
Dept. of Information Engineering, Niigata University
Ikarashi 2-8050, Niigata-shi 950-2181, Japan
Email : murase@wave.ie.niigata-u.ac.jp

1. Introduction

Tree canopies contain various scattering elements such as leaves, branches, and trunks, which contribute to complex backscatter, depending on frequency and polarization [1]-[4]. It is necessary to examine the fundamental scattering behavior to interpret remotely sensed data. In this paper, we tried to acquire fully polarimetric data of a small tree in the X-band. Since the range resolution of radar depends on the bandwidth of transmitted signal, we used 2 GHz bandwidth for high resolution imaging. After 3-D imaging, the three-component decomposition algorithm has been applied to extract fundamental scattering behavior. Then the scattering matrix along the range direction has been examined, which exhibits attractive changes of polarimetric signature along the range direction within the tree.

2. Experiment

To perform the radar imaging of a small tree (30 cm high, 8 cm wide), a 3-D imaging experiment was carried out in anechoic chamber as shown in Fig.1. The distance R from the antennas and the tree is 250 cm as shown Fig.2. The parameters of experiment are listed in Table I.

3. Polarimetric slice image

Fig.3 shows fully (LL, LR, LR) polarimetric images of the small tree after 2-D synthetic aperture processing [5]. It is seen in Fig.3 that there is no distinct difference in polarimetric channel. The backscattered powers in all polarimetric channel are almost the same. However, the RR channel power is large at the top of the tree.

4. Three-component decomposition image

If a scattering matrix [$\boldsymbol{S}$] is obtained, [$\boldsymbol{S}$] can be decomposed into three fundamental components [6], as follows :

$$[\boldsymbol{S}] = e^{j\phi}\{ e^{j\phi_s} K_s [\boldsymbol{S}]_{sphere} + K_d [\boldsymbol{S}]_{diplane} + K_h [\boldsymbol{S}]_{helix} \} . \qquad (1)$$

where the factors K_s , K_d , and K_h represent the magnitude contribution of single reflection, double reflection, and generation of circular polarization. The contribution of each component is determined by the ratio

$$\frac{K_i}{K_s + K_d + K_h} \qquad (i = s, d, h) \qquad (2)$$

After examining the value, we can examine the scattering behavior. Fig.4 shows the three-component images of a small tree. It is seen that K_s image in Fig.4 (a) is similar to K_d image (b), but K_h image (c) is fairly weak in comparison to K_s , and K_d components. Therefore, the single and double bounce components dominate in the tree at X-band.

5. Scattering matrix along range

It seems interesting to see how the scattering matrix changes along the range direction. The symbol #1 in Fig.5 indicates the slice position of the tree, #2 in the middle, and #3 in the back. By averaging out 1024 scattering matrices in each sliced plane through Mueller Matrix manipulation,

the relative scattering matrix has been obtained. Polarimetric signature in the Co-Pol channel are illustrated in Fig.6 (a)-(c). It is seen that polarimetric signature changes according to position #1, #2, and #3. Since the range resolution is 7.5 cm in this experiment, and the spacing between #1 and #2 is 8 cm, the neighboring sliced plane image is independent from the view point of range resolution. The result of Fig.6 (a)-(c) indicates multiple scattering occurs as we look deeper in the tree.

A polarimetric signature in Fig.6 (d) is derived from a sum of scattering matrix at #1, #2, and #3 silced plane. From illustrated polarimetric signature in Fig.6 (d), it is seen that a small trees has strong reflection of plate component.

6. Conclusion

We carried out a polarimetric 3-D imaging of a small tree. Using of 2-D synthetic aperture processing data, a wealth of polarization information has been used to obtain each image. These images can provide data for understanding fundamental scattering behavior of tree components.

Acknowledgement

This work in part was supported by Grant in Aid for scientific Research, Ministry of Education, Japan.

References

[1] E. Mougin, A. Lopes, M. A. Karam and A. K. Fung, "Effect of tree structure on X-band microwave signature of conifers," *IEEE Trans. Geosci. Remote Sensing*, vol. 31, pp. 655 - 667, May 1993.

[2] S. C. M. Brown, and J. C. Bennet, "High-resolution microwave polarimetric imaging of small trees," *IEEE Trans. Geosci. Remote Sensing*, vol. 37, pp. 48-53, Jan. 1999.

[3] J. Fortumy and A. J. Sirber, "Three-dimensional synthetic aperture radar imaging of a fir tree: First results," *IEEE Trans. Geosci. Remote Sensing*, vol. 37, pp 1006-1014, Mar. 1999.

[4] S. R. Cloude, J. Fortuny, J. M. Lopez-Sancdez and A. J. Sieber, "Wide-band polarimetric radar inversion studies for vegetation layers," *IEEE Trans. Geosci. Remote Sensing*, vol. 37, pp. 2430-2441, Sept. 1999.

[5] Y. Yamaguchi, T. Nishikawa, M. Sengoku, W. -M. Boerner, "Two-dimensional and full polarimetric imaging by a synthetic aperture FM-CW radar," *IEEE Trans. Geosci. Remote Sensing*, vol. 33, pp. 421-427, Mar. 1995.

[6] E. krogager, Z. H. Czyz, "Properties of the sphere, diplane, helix decomposition," in *Proc. 3rd Int. Workshop Radar polarimetry*, vol. 1, pp. 106 - 114, Mar. 1995.

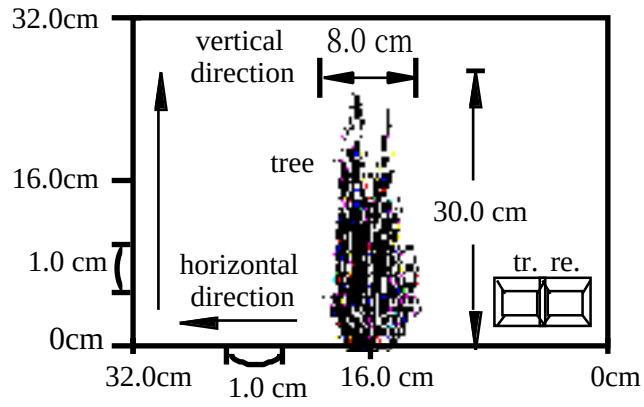

Fig. 1 Mesurement diagram viewed from anttena.

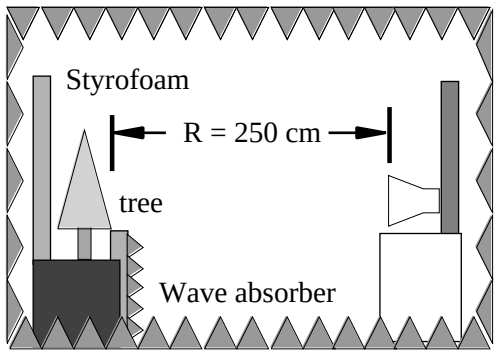

Fig. 2 Imaging geometry of a small tree.

Table I Parameters of experiment.

system	Network analyzer (HP8720C)
antenna	Rectangular horn
polarizations	HH, HV, VV
frequency point	401 points
sweep frequency range	9.0 - 11.0 GHz
scanning area	32 x 32 cm^2
scanning interval	1.0 cm

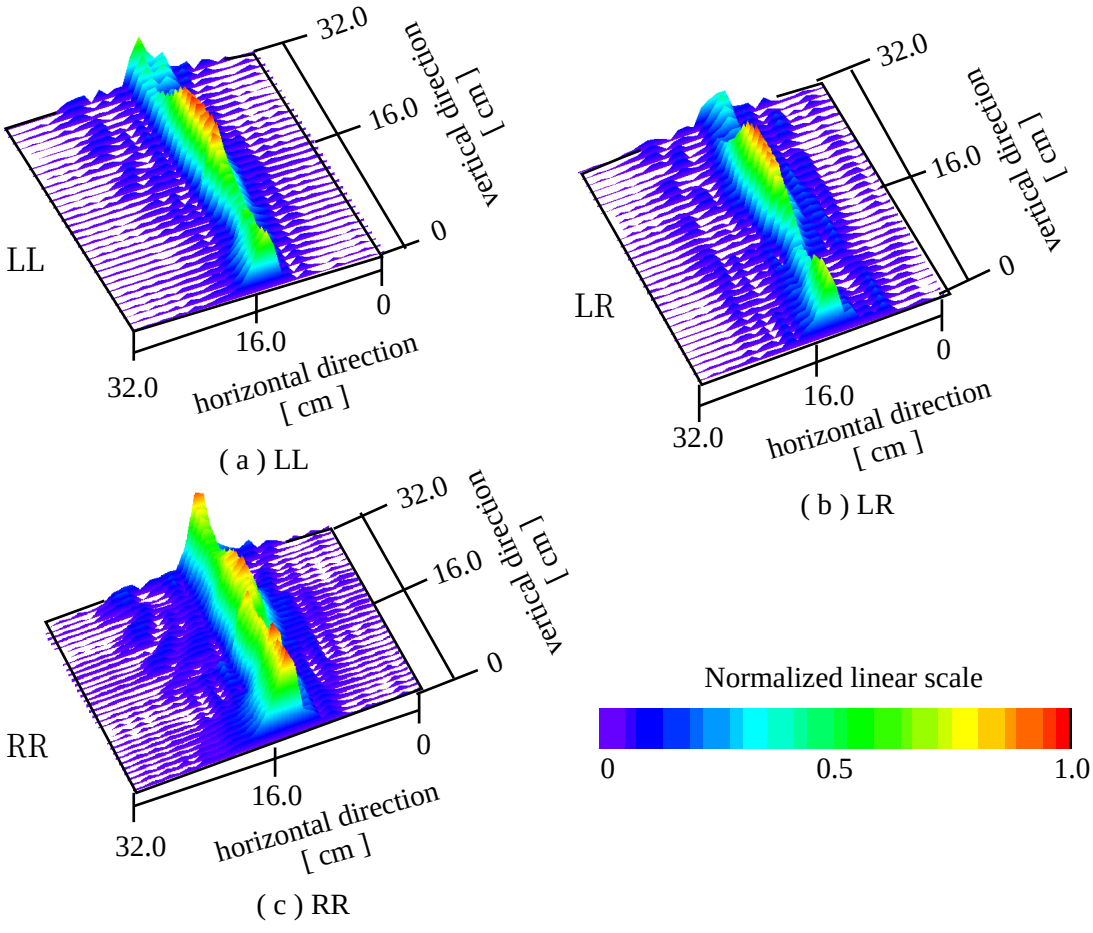

Fig. 3 A small tree images power in the LR polarization basis.

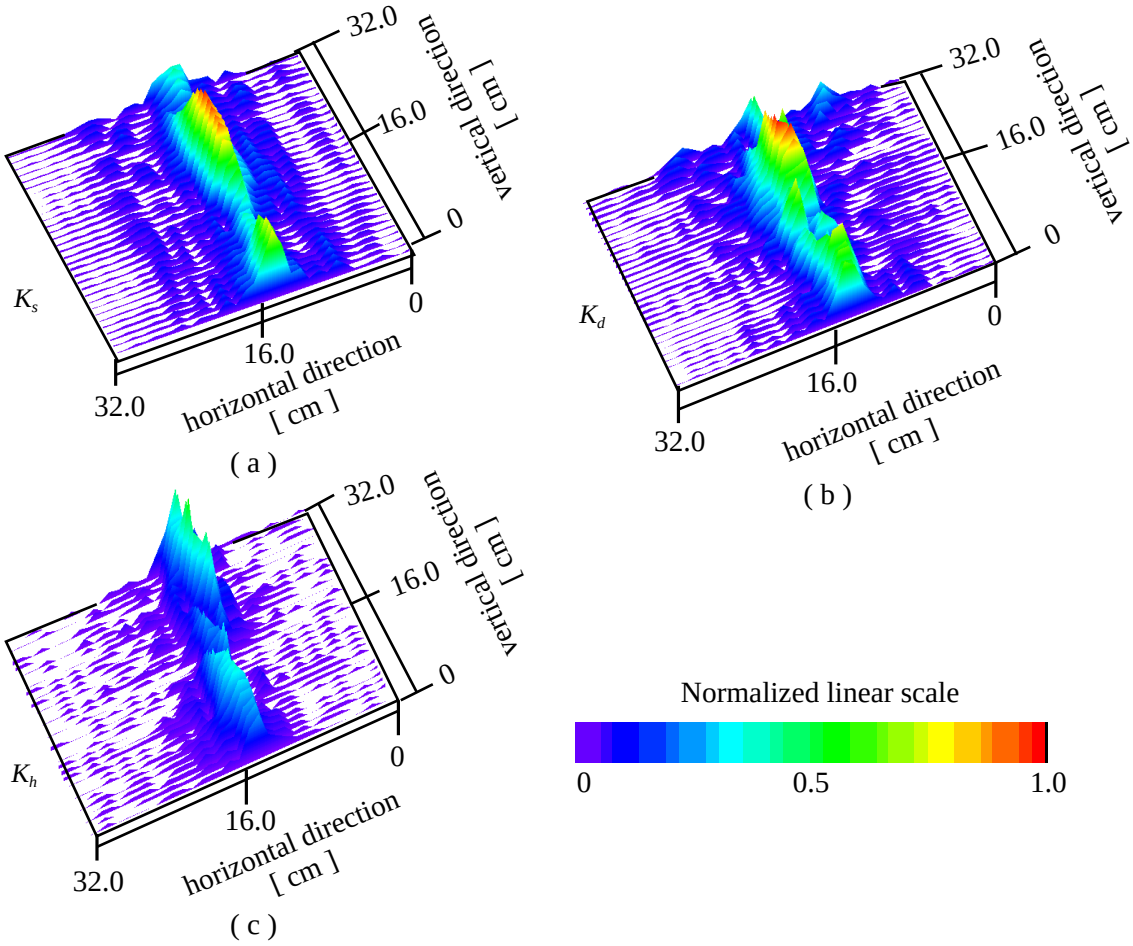

Fig. 4 Three component decomposition images : (a) K_s , (b) K_d , (c) K_h .

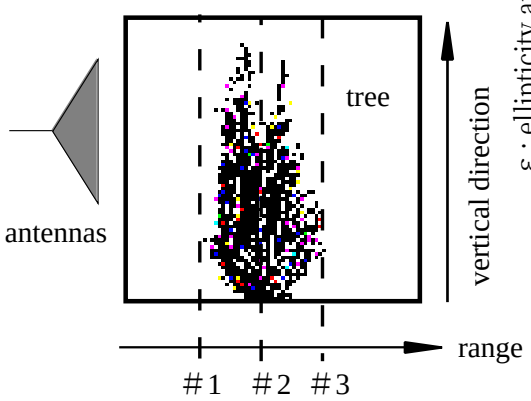

Fig. 5 A geometry of slice plane along range direction

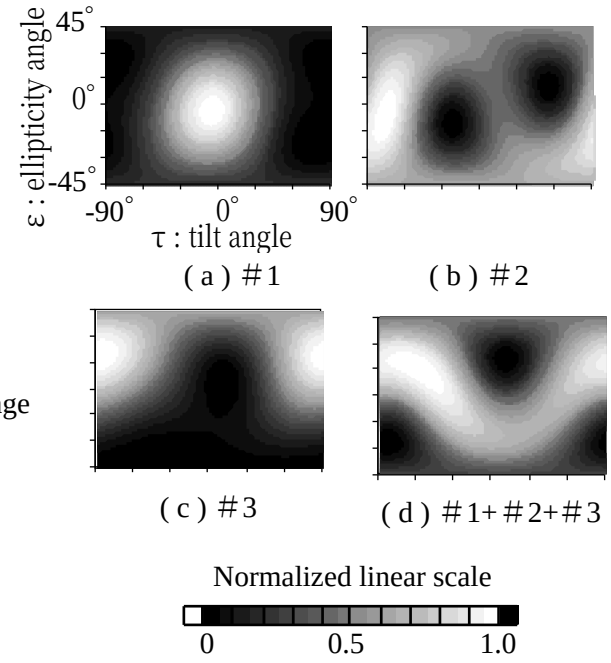

Fig. 6 Polarimetic signature of slice plane along range direcoin